NASA

Technical Memorandum 82019

A Physical Basis for Remote Rock Mapping of Igneous Rocks Using Spectral Variations in Thermal Infrared Emittance

Louis S. Walter and Mark L. Labovitz

OCTOBER 1980

National Aeronautics and Space Administration

Goddard Space Flight Center
Greenbelt, Maryland 20771

TM 82019

A PHYSICAL BASIS FOR REMOTE ROCK MAPPING OF IGNEOUS ROCKS USING SPECTRAL VARIATIONS IN THERMAL INFRARED EMITTANCE

By
Louis S. Walter
and
Mark L. Labovitz
Applications Directorate

October 1980

GODDARD SPACE FLIGHT CENTER
Greenbelt, Maryland 20771

A PHYSICAL BASIS FOR REMOTE ROCK MAPPING OF IGNEOUS ROCKS USING SPECTRAL VARIATIONS IN THERMAL INFRARED EMITTANCE

Louis S. Walter and Mark L. Labovitz
Applications Directorate
Goddard Space Flight Center
Greenbelt, Maryland 20771

ABSTRACT

The thermal infrared spectra of rocks are potentially of considerable importance for remote sensing. This paper presents results of a theoretical investigation of the relation between spectral features in the 8–12 micrometer region and rock type. Data on compositions of a suite of rocks and measurements of their spectral intensities in 8.2–10.9 and 9.4–12.1 micrometer bands published by Vincent (1973) were subjected to various quantitative procedures. It was found that there was no consistent direct relationship between rock group names and between the Thornton–Tuttle (1960) Differentiation Index and the relative spectral intensities. This relationship is explicable on the basis of the change in average Si–O bond length which is a function of the degree of polymerization of the SiO_4 tetrahedra of the silicate minerals in the igneous rocks.

A PHYSICAL BASIS FOR REMOTE ROCK MAPPING OF IGNEOUS ROCKS USING SPECTRAL VARIATIONS IN THERMAL INFRARED EMITTANCE

INTRODUCTION

The use of infrared spectroscopy for the remote characterization of planetary and terrestrial surfaces has received some interest due to efforts in the investigation of these bodies from space. The interested reader is referred to works such as those by Karr (1975) and Smith (1977) for some examples of these studies.

Much of the emphasis in this work has been on the reflectance properties of rocks in the near infrared (up to 2.5 μm) because the energy available in this reflective region of the spectrum is much greater than that at longer wavelengths. However, a depression in the thermal infrared emittance spectra of rocks (sometimes called restrahlen) is related to the sympathetic vibration of Si–O bonds. Shifts in the location of this feature have been ascribed to variations in rock-type. This concept has spurred researchers such as Logan, Hunt and Salisbury (1975) and Lyon and Green (1975) to investigate the relationships of the position of the emittance depression with respect to rock composition.

In order to explore the utility of using this spectral variation for remote discrimination of rock types, NASA launched the Surface Composition Mapping Radiometer (SCMR) aboard the Nimbus-5 spacecraft in 1972. This instrument had two spectral bands centered at 8.8 and 10.7 μm; variation in the relative intensities of these bands was to be correlated with variation in rock composition. Unfortunately, the instrument did not produce a great deal of data. However, there was some indication that these data could be used for rock discrimination (Lyon and Green, 1975; Walter et al., 1976).

Previous studies of the relationship between variations in spectral intensity in the thermal infrared and rock type have been largely empirical Vincent (1972) attempted to correlate the variation with silica content, but SiO_2 abundance by itself is notoriously poor as an indicator of rock type. He later presented a broader, but still empirically-based analysis of the problem (Vincent, 1973). We attempt here to derive statistically acceptable correlations between spectral variations and the variations in the chemistry (and normative mineralogy) of rocks and to develop a rudimentary phenomenological model for the variation in terms of mineralogical variations in rocks. From this, it is possible to develop a crude relationship between spectral variations and rock-type which may be useful for rock-classification by remote sensing from space.

The work presented here is based on laboratory measurements of igneous rock spectra published by Vincent (1973) together with corresponding chemical analyses and calculations of normative mineralogy. The twenty-five samples analyzed covered a fiarly broad distribution of major igneous rock types, but unfortunately, for many of these types there were no replicate samples. The spectral variation was characterized as the ratio ($R_{1,2}$) of spectral intensities in a band from 8.2–10.9 μm relative to a band from 9.4–12.1 μm. Sometime ago, Lyon (1964) showed that this ratio increases as the rocks become more basic (less silicic).

Using these data, reproduced in Table 1, an attempt has been made to determine the major cause of this spectral change and relate this to some parameter which can be used to characterize igneous silicate rocks.

Since the results of the analyses discussed below are used to make inferences to a larger population, it would be well for the reader to keep in mine that the 25 rock samples are igneous rocks. Further the proportions of the various rocks in the suite are not by implication considered to be representative of any specific location on the earth's surface. Vincent (1973) originally read this suite because of the wide range of textures and compositions represented. Therefore, the relationships developed within this paper are not necessarily applicable to metamorphic or sedimentary rocks. Proof of the

Table 1
Data Used in This Work (from Vincent, 1973)
a) $R_{1,2}$ and Chemical Data (wt. %)

Sample No.	Sample Name	$R_{1,2}$	SiO_2	Al_2O_3	Fe_2O_3	FeO	MgO	CaO	Na_2O	K_2O	H_2O	TiO_2	P_2O_5	MnO	CO_2
1	Granite	1.1761	76.7	12.8	0.49	< .05	0.15	0.11	4.5	4.3	0.39	0.06	.01	.02	< .05
2	Granite	1.1946	68.2	16.5	0.82	2.8	1.1	2.6	3.9	4.9	0.72	0.53	.16	.08	< .05
3	Granite	1.1987	72.4	14.2	0.88	1.2	0.31	1.2	3.6	5.0	0.74	0.20	.04	.06	< .05
4	Rhyolite	1.1266	75.1	11.5	1.8	0.80	0.23	0.51	4.0	4.4	1.40	0.25	.04	.00	< .05
5	Rhyolite (Welded Tuff)	1.1741	76.1	12.1	1.0	0.56	0.15	0.21	3.5	4.6	1.57	0.12	.00	.00	< .05
6	Pyroxene Syenite	1.1784	61.4	20.3	1.6	0.52	0.24	0.99	3.6	9.7	0.86	0.22	.03	.04	0.21
7	Trachyte (Porphyritic)	1.1442	68.3	17.7	1.0	0.60	0.26	0.31	4.8	5.1	0.82	0.24	.03	.13	0.24
8	Nepheline Syenite	1.2094	58.3	19.7	1.9	1.3	0.53	1.5	7.4	6.4	0.98	0.82	.09	.30	< .05
9	Granodiorite	1.2134	53.6	18.7	1.3	7.0	3.8	6.2	3.9	2.8	1.20	0.99	.18	.17	< .05
10	Granodiorite	1.1723	62.8	16.0	0.64	1.6	0.90	1.8	3.9	4.4	0.99	0.56	.09	.04	< .05
11	Dacite	1.1724	65.7	15.0	1.2	1.3	1.5	3.0	3.9	3.4	1.24	0.35	.16	.04	2.70
12	Dacite	1.1436	66.9	15.3	1.1	1.6	1.4	3.8	3.8	2.4	2.02	0.59	.14	.00	0.21
13	Dacite	1.1574	67.0	16.0	1.6	1.6	1.8	2.1	4.1	2.8	2.07	0.63	.16	.00	< .05
14	Diorite	1.1685	61.0	16.4	1.8	5.6	1.4	4.6	4.3	2.5	1.00	0.92	.36	.16	< .05
15	Diorite	1.1795	56.2	17.4	1.8	5.4	4.4	7.1	3.9	1.8	0.71	0.84	.29	.12	< .05
16	Andesite	1.1962	57.8	15.2	2.2	3.3	5.0	5.5	3.2	1.8	2.40	0.51	.20	.09	2.60
17	Rhyolite	1.1394	67.9	14.5	1.8	0.40	0.53	1.1	0.59	10.0	1.71	0.44	.09	.02	0.38
18	Gabbro	1.1810	50.6	15.7	4.0	6.5	6.9	10.7	2.4	0.70	0.94	0.86	.12	.17	< .05
19	Basalt	1.2154	47.5	16.3	2.2	7.9	7.9	8.9	3.7	1.6	0.74	2.10	.62	.13	< .05
20	Basalt	1.2204	48.0	15.1	2.9	7.6	9.4	9.5	3.2	1.1	0.74	1.80	.60	.12	< .05
21	Basalt	1.2246	48.4	16.6	2.2	8.0	7.3	9.4	3.5	1.3	0.55	2.00	.51	.13	< .05
22	Basalt	1.2255	48.3	16.5	1.6	8.6	7.6	8.1	3.7	1.7	0.71	2.30	.73	.13	< .05
23	Basalt	1.2018	47.8	16.9	2.1	8.1	6.2	10.1	3.1	1.0	0.97	1.90	.38	.12	0.76
24	Anorthosite	1.2468	49.7	28.3	0.84	1.6	1.5	13.9	2.5	0.13	0.71	0.30	.02	.00	< .05
25	Diabase	1.2204	52.4	15.0	1.1	8.5	7.1	10.7	2.0	0.64	1.21	1.00	.13	.13	< .05
26	Peridotite	1.3723	44.5	1.5	0.23	7.7	43.3	1.8	0.13	0.08	0.66	0.10	.04	.07	< .05

Table 1 (Continued)

b) $R_{1,2}$ and Normative Mineral Data (wt. %) (Cont'd)

Sample No.	Sample Name	CLFA	HEM	MAG	ILM	APA	CAL	COR	WAT	NEPH	WOL
1	Granite (A79)		0.23	0.03	0.06	0.02	0.11	0.45	1.03		
2	Granite (A119)			0.61	0.57	0.31	0.11	0.37	1.66		
3	Granite (A122)			0.65	0.21	0.09		0.52	1.94		
4	Rhyolite (SA-49)		0.16	0.93	0.26	0.06	0.11		3.64		
5	Rhyolite (Weld. Tuff)			0.72	0.13		0.11	0.71	4.06		
6	Pyroxene Syenite (E83A)		0.39	0.60	0.23	0.06	0.46	1.74	2.25		
7	Trachyte			0.74	0.25	0.06	0.53	2.89	2.17		
8	Neph. Syenite			1.40	0.87	0.17	0.11		2.58	14.12	0.47
9	Granodior. (A117)	1.99		1.01	1.12	0.20	0.11		0.95		
10	Granodior. (A127)			0.47	0.60	0.19	1.25	2.62			
11	Dacite (E12A)			0.90	0.38	0.32	6.07	4.12	3.32		
12	Dacite (2A1)			0.81	0.63	0.27	0.46	0.24	5.30		
13	Dacite (2B5)W			1.19	0.67	0.31	0.11	1.93	5.47		
14	Diorite (A129)			1.38	1.02	0.61	0.12		2.75		
15	Diorite (E470)			1.42	0.96	0.60	0.12		2.00		
16	Andesite (E55A)			1.66	0.56	0.40	0.60		6.48		
17	Rhyolite (2A3)		0.86	0.04	0.46	0.17	0.82	1.17	4.43		
18	Gabbro (E80A)			3.29	1.02	0.26	0.12		2.76		
19	Basalt (1A8)	3.80		1.80	2.46	1.34	0.12		2.16	4.75	
20	Basalt (WI-1-109)	3.53		2.39	2.15	1.30	0.12		2.19	0.38	
21	Basalt (S95)	3.85		1.81	2.38	1.10	0.12		1.61	1.75	
22	Basalt (584)	u	u	u	u	u	u	u	u	u	u
23	Basalt (1A3)	2.66		1.71	2.23	0.81	1.85		2.82		
24	Anorthosite (AN)			0.65	0.33	0.04	0.12		1.95		
25	Diabase			0.90	1.18	0.28	0.12		3.54		
26	Peridotite (EP-1)	6.74		0.21	0.13	0.10			1.82		

QTZ = quartz
ORTHO = orthoclase
ALB = albite
ANOR = anorthite
CPWO = $Wollastonite_{SS}$
CPEN = $Enstatite_{SS}$
CPFS = $Ferrosilite_{SS}$
OPEN = $Enstatite_{SS}$
OPFS = $Ferrosilite_{SS}$
OLFO = olivine (fosterite)
OLFA = olivine (fayelite)
HEM = hematite
ILM = ilmenite
APA = apatite
CAL = calcite
COR = corundum
WAT = water
NEPH = nepheline
WOL = wollastonite

u = unmeasured

Table 1 (Continued)

b) $R_{1,2}$ and Normative Mineral Data (wt. %)

Sample No.	Sample Name	$R_{1,2}$	QTZ	ORTHO	ALB	ANOR	CPWO	CPEN	CPFS	OPEN	OPFS	OLFO
1	Granite (A79)	1.1761	33.34	25.87	38.03	0.16				0.31		
2	Granite (A119)	1.1946	16.67	30.20	33.77	11.21				2.30	2.49	
3	Granite (A122)	1.1987	28.64	30.27	30.61	5.43				0.64	0.83	
4	Rhyolite (SA-49)	1.1266	33.50	26.02	33.60	0.40	0.55	0.44		0.02		
5	Rhyolite (Weld. Tuff)	1.1741	36.68	27.34	29.22	0.68				03.0		
6	Pyroxene Syenite (F83A)	1.1784	0.49	58.37	30.43	3.21				0.49		
7	Trachyte	1.1442	20.44	31.01	40.99					0.54	0.08	
8	Neph. Syenite	1.2094		38.70	36.99	1.56	1.31	1.06	0.02			
9	Granodior. (A117)	1.2134		17.97	35.14	25.53	1.50	0.67	0.67	4.40	3.88	2.22
10	Granodior. (A127)	1.1723	17.75	26.81	33.38	7.70				1.86	1.03	
11	Dacite (E12A)	1.1724	29.11	20.96	33.77					3.14	0.60	
12	Dacite (2A1)	1.1436	25.59	14.47	32.18	15.78				2.87	0.69	
13	Dacite (2B5)	1.1574	25.50	17.01	34.98	8.67				3.72	0.38	
14	Diorite (A129)	1.1685	13.01	15.80	38.18	17.99	0.92	0.29	0.56	2.71	4.70	
15	Diorite (E47C)	1.1795	4.57	11.68	35.53	25.20	3.50	1.73	1.04	7.92	4.19	
16	Andesite (E56A)	1.1962	13.51	11.18	27.91	21.33	0.94	0.62	0.16	9.91	3.25	
17	Rhyolite (2A3)	1.1394	23.75	59.47	4.92	2.31				1.07		
18	Gabbro (E80A)	1.1810	2.82	4.73	22.80	31.97	8.70	5.35	2.13	10.36	3.62	
19	Basalt (1A8)	1.2154		10.76	26.22	24.52	6.55	3.93	1.72			9.75
20	Basalt (WI-1-109)	1.2204		7.47	29.22	25.23	7.65	4.89	1.67			11.60
21	Basalt (S95)	1.2246		8.77	29.95	27.37	6.80	3.96	1.94			8.82
22	Basalt (5B4)	1.2255	u	u	u	u	u	u	u	u	u	u
23	Basalt (1A3)	1.2018		6.68	29.09	30.79	5.29	2.89	1.74	3.97	2.10	4.97
24	Anorthosite (AN)	1.2458	2.75	0.82	22.17	65.27	1.07	0.65	0.27	2.55	0.95	
25	Diabase	1.2204	4.39	4.31	18.91	31.89	8.60	4.49	3.07	11.62	6.96	
26	Peridotite (EP-1)	1.3723		0.60	1.36	3.84	2.26	1.75	0.21	14.89	1.53	64.57

u = unmeasured

utility of procedures and conjectures described below for identifying such rocks as well as for specific spatial arrangements and proportions of rocks awaits further experimentation.

RELATIONSHIP OF $R_{1,2}$ TO ROCK NAME

Before proceeding, it would be wise to determine whether or to what degree $R_{1,2}$ can be used to characterize, or act as a surrogate measure of, the relatively subjective classification given to hand specimens by a group of collectors. To test this hypothesis, the names bestowed upon the 25 igneous rocks by the geologist who collected them, were grouped as per Table 2. The analysis was performed by testing to see if there are significant differences in the $R_{1,2}$ means of the groups. Accepting an hypothesis that claims there are significant differences in the means of the groups implies that the $R_{1,2}$ value might be used to differentiate rocks which were largely identified in hand specimen. The procedure used to test hypotheses of this nature is called analysis of variance (Fisher, 1970). Anorthite, diabase and peridotite were not used in this analysis because they represent one-member groups. The results of the analysis of variance (Table 3) were obtained using the MINITAB2 statistical package (Ryan et al., 1976). The F-Ratio is not significant at any conventional significance level and thus there is no evidence to indicate that these samples so grouped can be differentiated using $R_{1,2}$. The large amount of overlap in the confidence limits illustrated in Figure 1 graphically indicates the lack of significant difference between the means.

Table 2
Groupings of rock names for use in analysis of variance.

Group 1	Group 3	Group 6
Granite (A79)	Granodiorite (A117)	Andesite (E55A)
Granite (A119)	Granodiorite (A127)	Andesite (2A3)
Granite (A122)		
Rhyolite (SA-49)	Group 4	Group 7
Rhyolite	Dacite (E12A)	Gabbro (E80A)
	Dacite (2A1)	Basalt (1A8)
Group 2	Dacite (2B5)W	Basalt (WI-1-104)
Pyroxene Syenite (A83E)		Basalt (S95)
Trachyte	Group 5	Basalt (5P4)
Nepheline Syenite	Diorite (A129)	Basalt (1A3)
	Diorite (E47C)	

Table 3

Analysis of variance, test of significant difference among means of groups of samples.

DUE TO	DF	SUM OF SQUARES	MEAN SQUARE	F*	P(F > F*)
GROUPINGS	6	0.008079	0.001346	2.19	0.10
ERROR	16	0.009832	0.000615		
TOTAL	22	0.017911			

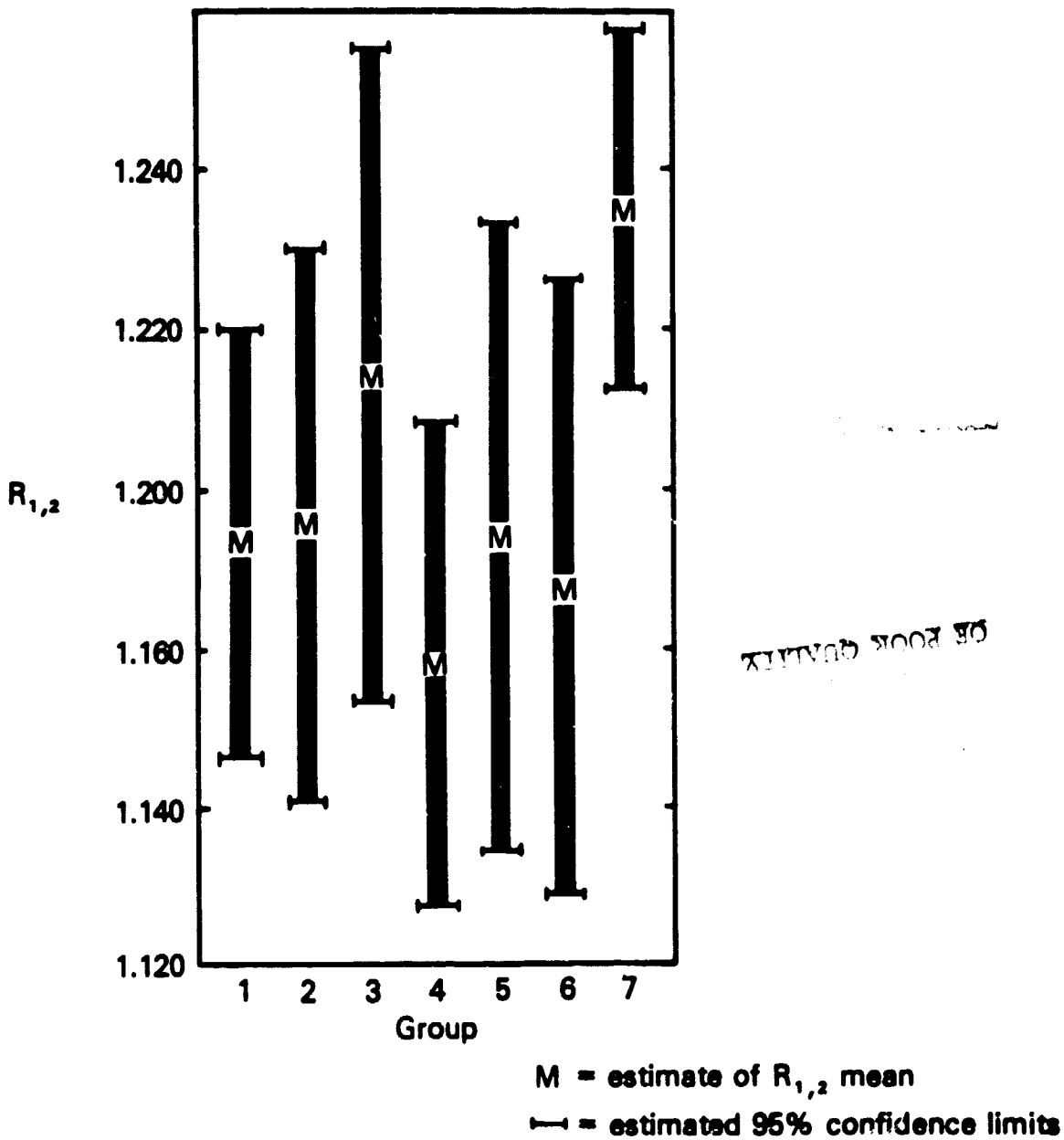

Figure 1. Individual 95 Percent Confidence Interval for Group Means (Based on Pooled Standard Deviations).

ANALYSIS STRATEGY

The two related sets of data obtained by Vincent (1972) were examined to determine the functional relationship (if any) between each of these data sets and the ratio $R_{1,2}$. The data sets, obtained from a suite of 25 igneous rock samples, were, 1) the weight percentage of 13 major elemental oxides (hereafter called "elemental data"); and 2) the weight percentage of 20 normative materials (hereafter called "mineralogical data"). The two data sets were not independently measured as the mineralogical data was derived from the elemental oxide data using a computer program devised by Rodgers et al., 1970. The values of the elemental data, the mineralogical data and $R_{1,2}$ for each rock sample have been reproduced in Table 1.

We have adopted the common statistical terminology designating the two compositional data sets as the independent or predictor variables and the ratio $R_{1,2}$ as the dependent or criterion variable. Through examination of each of the compositional data sets in turn, we attempted to establish a function which relates members of each of these sets to the corresponding criterion variable. These functions were to be parsimonious (Draper and Smith, 1966), i.e., have as few parameters as possible, while being subject to the constraint of an adequate statistical fit and consistent with theoretical considerations.

The number of predictor variables must be reduced in order to 1) have sufficient degrees of freedom to perform a sensitive test of significance; 2) to avoid "artifacts" in the analysis such as overly optimistic estimates of diagnostic analysis statistics which can occur as the result of the inclusion of redundant or irrelevant variables (Draper and Smith, 1966); and 3) to reduce the influence of ratio correlations (Chayes, 1971) arising from having a predictor set whose values sum to a constant (in this instance, each case sums to 100 percent).

The number of predictor variables was reduced in two steps. The first step used information which came strictly from the predictor data set; the objective being to reduce redundancy among the predictor variables. The procedure involved extraction of components of the correlation matrix; predictors which "load" strongly on the same component vary similarly across the sample space (Gorsuch, 1974). Because the method used for component extraction yields orthogonal components, variables loading highly on different components represented different patterns of variations and it is possible to reduce redundancy by selecting only one variable representing each pattern of variation. When there was a choice among more than one variable, theoretical considerations were used to guide the selection. The SPSS subprogram FACTOR (Kim, 1975) selecting options PA1, and PA2 and a VARIMAX rotation was used as implemented on an IBM 370/3033 at the Pennsylvania State University. In the second step, the subset of predictor variables arising from the components analysis was input along with $R_{1,2}$ values to an All-Possible-Subsets-Regression (Neter and Wisserman, 1974; Draper and Smith, 1966). This procedure evaluates regressions of the criterion upon all combinations of the predictor variables. There are $\sum_{r=1}^{p'} \binom{p'}{r}$ regressions evaluated, where: p' is the number of predictors arising from step 1, and $\binom{p'}{r} = p'!/(p'-r)!r!$. For example, in the case $p' = 5$, 31 regressions would be evaluated (5 with one predictor, 10 with two predictors, 10 with three predictors, 5 with four predictors, and one with all five predictors). The regressions are evaluated by examining functions of the regression sum of squares (SSR), the error sum of squares (SSE), and plots of the residuals which are departures of the observed values of $R_{1,2}$ from their expected values. The program used to perform this analysis was the P9R program of the BMD system (Frane, 1979) using the Furnival and Wilson (1974) search procedure and R^2_{ADJ} (defined as R^2 adjusted for the number of degrees of freedom) and Mallow's C_p (Daniel and Wood, 1971) as the evaluation criteria.

RESULTS

Elemental Data

For the elemental data, in step 1, only phosphorous could be removed from consideration. The element had a greater than 80 percent (94.2) loading along with titanium (89.6) on component 1. Because silica represents the most dominant variable (having a mean of about 60% by weight), analyses were performed both with and without silica in the subset. This was done to determine what fine detail, if any, is being hidden by the presence of silica.

For either subset (with or without silica) the R^2_{ADJ} and C_p criteria are both optimized when the 5 elements Ca, K, Mg, Na, Fe^{+3} are the predictor variables. However, analysis of the residuals indicate that the peridotite value is an outlier and resulting in spuriously high coefficients of correlation (R=0.95) and determination (R^2=0.90 and R^2_{ADJ}=0.876)

With peridotite removed from the analysis, the subset without silica achieves the lowest C_p value when Al, Mg and Fe^{+3} are in the equation. In the previously-cited analysis (with the peridotite included), Al, Mg and Fe^{+3} provide the best regression if the number of independent variables used is restricted to three. Salient statistics from this regression equation are given in Table 4.

Table 4
Statistics for elemental data -- SiO_2 and P_2O_5 not included.

Mallows' C_p	0.56
Squared Multiple Correlation, R^2	0.685
Multiple Correlation, R	0.828
Adjusted Squared Mult. Corr., R^2_{ADJ}	0.638

Variable Name	Regression Coefficient	Standard Error	Standard Coefficient	T*	P(T>|T*|)	Contribution to R-Squared
Intercept	1.10993	0.021564	36.484	51.47	0.000	
Al	0.00462	0.001164	0.500	3.97	0.001	0.248
Mg	0.00844	0.001689	0.837	4.99	0.000	0.392
Fe^{+3}	-0.01551	0.006472	-0.403	-2.40	0.026	0.090

When silica is included in the analysis (no peridotite), it replaces Al and Mg in the subset of independent variables forming the best regression equation (Table 5).

The influence of Si in terms of explanatory power is equal to but opposite in "effect" to that of Al and Mg. Comparison of the results in Tables 4 and 5 indicates that the explanatory power (estimated by R^2_{ADJ}) of the two models is roughly equal, while the coefficients of Fe^{+3} in the two models are not significantly different from one another. Thus, the variation explained by Mg and Al is equal to that explained by Si. The inverse relationship between Al-Mg and Si can be seen in the opposite signs for the coefficients of Al-Mg (positive values) and Si (negative value). Consequently, the value of $R_{1,2}$ decreases with increasing Si, or with decreasing Al + Mg. Analysis of the residuals gives no evidence to reject the hypothesis that they are normally and independently distributed.

Mineralogical Data

Because there are 20 minerals in this predictor set with only 25 samples, the number of independent variables being considered must be reduced to permit formulation of a regression model. With the

Table 5
Statistics for elemental data – P_2O_5 not included.

Mallows' C_p	-0.37
Squared Multiple Correlation, R^2	0.646
Multiple Correlation, R	0.804
Adjusted Squared Mult. Corr., R^2_{ADJ}	0.613

Variable Name	Regression Coefficient	Standard Error	Standard Coefficient	T*	P (T>|T*|)	Contribution to R-Squared
Intercept	1.39725	0.367926	45.929	37.98	0.000	
Si	-0.00305	0.000498	-0.963	-6.13	0.000	0.632
Fe^{+3}	-0.01638	0.006050	-0.426	-2.71	0.013	0.124

component – factor analysis of step 1, the number of predictors was reduced from 20 to 12. The variables selected are in bold face in the canonical form of the pattern matrix given in Table 6.

Initial runs of the step 2 analysis, led to discarding nepheline syenite and peridotite as outliers because of their large Mahalanobis D^2 values. Wollastonite had to be dropped from the predictor subset because it occurred in only the nepheline syenite sample.

Two regression equations emerged from the analysis. The regression containing the independent variables forsterite, anorthite and water is statistically stable in that it emerges as the best (or nonsignificantly different from the best) subset regardless of the presence or absence from the sample of nepheline syenite or peridotite. This regression also has the optimal Mallows' C_p value of those models drawn from a subset of the predictor variables defined below. Summary statistics are given in Table 7.

Table 6
Factor pattern matrix for mineralogical data.

	F1	F2	F3	F4	F5	F6	F7
CPWO	0.909						
CPEN	0.895						
CPFS	0.879						
ILM	0.920						
APA	0.832						
MAG	0.756						
QTZ	-0.607						
ANOR	0.531						
ORTHO	-0.462				-0.648		
OLFO		0.983					
OLFA		0.856					
ALB		-0.644			0.514		
OPEN			0.861				
OPFS			0.760				
NEPH				0.945			
WOL				0.983			
HEM					-0.888		
CAL						0.783	
COR						0.852	
WATER							0.883

Table 7
Statistics from regression of water, forsterite and anorthite.

Mallows' C_p	2.56
Squared Multiple Correlation, R^2	0.69776
Multiple Correlation, R	0.83532
Adjusted Squared Mult. Corr., R^2_{ADJ}	0.65004

Variable Name	Regression Coefficient	Standard Error	Standard Coefficient	T*	P(T>|T*|)	Contribution to R-Squared
Intercept	1.17277	0.00956622	38.237	122.59	0.000	
WAT	-0.00452227	0.00255464	-0.230	-1.77	0.093	0.049849
OLO	0.00232985	0.00116707	0.269	2.00	0.060	0.063395
AN	0.00124317	0.000256475	0.640	4.85	0.000	0.373736

The second predictor subset includes orthopyroxene, quartz, forsterite, clinopyroxene, oral (a summed combination orthoclase and albite) anorthite and water. It yielded a model containing oral, orthopyroxene and quartz (with the results for olivine leading us to an uncertain conclusion as to its significance). Statistics from this regression are given in Table 8. The order of "importance" of the variables, using the contribution to R^2 as the importance criterion, is quartz, alkali feldspar, pyroxene and olivine.

Table 8
Statistics from regression of oral (orthoclase+albite), orthopyroxene and quartz.

Squared Multiple Correlation, R^2	0.609
Multiple Correlation, R	0.780
Adjusted Squared Mult. Corr., R^2_{ADJ}	0.547

Variable Name	Regression Coefficient	Standard Error	Standard Coefficient	T*	P(T>|T*|)	Contribution to R-Squared
Intercept	1.25502	0.019532	40.919	64.25	0.0	
ORAL	-0.00090	0.000347	-0.479	-2.61	0.017	0.140
OPE	-0.00213	0.001476	-0.247	-1.44	0.165	0.043
QTZ	-0.00126	0.000384	-0.537	-3.30	0.004	0.223

INTERPRETATION

The decreased emittance of silicate rocks in the region from 9 to 11 μm is known to be due to the sympathetic vibration of the stretching of the silicon–oxygen bonds at these wavelengths. The frequency (at ca. 1000 cm^{-1}) is directly related to the force by which the silicon and oxygen ions are bonded together; the greater the force, the higher the frequency of the sympathetic vibration and thus the shorter the wavelength at which one observes the decreased emittance. The oxygen of the Si–O couple is shared by another cation (Si–O–X) and the force of the Si–O bond is affected by that of the O–X bond. Thus, the shape and location of the depression can change.

Three types of effects on the Si–O bond may be considered: substitution, disordering and polymerization. Substitution effects are the result of replacement of one cation by another in a single mineral species (e.g., Fe by Mg in orthopyroxene). Replacement of large cations by cations with smaller ionic radii causes the frequencies of the sympathetic vibrations of the Si–O bond to decrease. This, in turn, results in an increase in the wavelength of Si–O absorbtion (Farmer, 1974). [It is, perhaps, more appropriate to consider the relationship between the location of the emittance depression and the electronegativity of the secondary cation (Strens, 1974)]. Disordering of cations within potential crystal sites also has an effect. For example, random substitutions of aluminum for silicon in feldspar results in an emittance minimum at higher wavelengths than if the same feldspar is ordered (Kovach et al., 1975). Polymerization of silica tetrahedra can be considered an extreme condition of ordering. It increases from the case of isolated tetrahedra (e.g., olivine) through chain silicates (e.g., pyroxene) and culminates in those cases in which the silica tetrahedra are all bound together in a framework (e.g., quartz and feldspar). The effect is such that in the progression from isolated to framework silicates, the depression in spectral emissivity which occurs at approximately

10 μm decreases in wavelength. In order to relate this shift in the emittance depression to the composition of minerals and rocks, it is first important to determine whether disordering, substitution or polymerization effects are the major cause of the shift.

Disordering can be ruled out immediately; this is an isochemical effect and thus cannot explain the variation of $R_{1,2}$ with chemistry as discussed in the previous section.

Two of the major monomineralic substitutions in minerals are those between iron and magnesium (in pyroxenes and olivines) and aluminum and silicon (in feldspars). In the previous section, it was shown that, insofar as this suite of igneous rocks is concerned, there is a positive correlation between the amount of aluminum and magnesium in them and the values for $R_{1,2}$. The centers of the two bands used to determine $R_{1,2}$ lie at 9.55 and 10.75 μm. The centers for the emittance depressions of these minerals (pyroxene, olivine and feldspar) lie between these band-center positions. Thus, for example, when ferrous iron substitutes for magnesium in a mineral, the wavelength of the emittance depression increases (Kovach et al., 1975) and the factor, $R_{1,2}$ (the ratio of the intensity of the low-wavelength band to that of the high wavelength band) should increase. The reverse seems to be the case; $R_{1,2}$ is positively correlated with total rock magnesium content. Likewise, the substitution of aluminum for silicon theoretically should reduce $R_{1,2}$ but we find that increased total aluminum content results in increased $R_{1,2}$.[1] These relationships provide a strong indication that solid substitution within mineral species is not the mechanism of the shift in $R_{1,2}$.

In chemical terms, the effect of polymerization on the position of the depression described above is consistent with the trend indicated in the previous section wherein $R_{1,2}$ increases (reflecting an

[1]This argument is based on the following assumptions which the authors consider to be warrented:
1. Substitutions of cations in mineral species mimics the variation of these cations in bulk rock chemistry;
2. The shapes of the curves at the emittance depressions do not differ greatly from one rock type to another.

increase in the wavelength of the emittance depression) as aluminum and magnesium increase and silicon decreases. Thus, $R_{1,2}$ increases from granite to basalt to peridotite as the position of the emittance depression increases in wavelength. This is also consonant with the results of the statistical analysis which indicate that quartz, alkali feldspar, pyroxene and olivine, in that order, are related to variation in $R_{1,2}$. Finally, this is consistent with the trend for the position of the emittance depression which increases from 9.2 to about 11 μm as we go from quartz to olivine.

In crystallographic terms, polymerization results in changes in the Si–O bond length and strength (Smith and Bailey, 1963) which, in turn, affects the $R_{1,2}$ factor. Brown and Gibbs (1969) related bond length and strength to the average cation coordination of oxygen in silicate minerals. These authors determined a linear relationship between the average coordination number, $\overline{CN}$ and the mean Si–O bond distance, $\overline{Si\text{–}O}$: $\overline{Si\text{–}O} = 0.015\ \overline{CM} + 1.579$ (units given in Ångstroms). Using this relationship, we can obtain values for the average Si–O bond distance for the whole rock by weighting each mineral average by its abundance relative to other silicates in each rock. The values for CN used for the major minerals were: quartz = 2.0; albite, orthoclase = 2.88; anorthite = 2.78; wollastonite, ortho- and clino-pyroxene = 3.33; olivine = 4.0 and nepheline = 2.83. These normative minerals account for over 90% of every rock in this suite. The total weighted average oxygen coordination number is plotted versus $R_{1,2}$ in Figure 2. Using all 25 samples for which Vincent (1973) gave normative analyses, the correlation coefficient, r, was found to be 0.86. These and other statistics[2]

[2] The slope, m, and intercept, c, of the simple linear regressions reported in Tables 9 and 10 were calculated using a procedure which minimizes the sum of squared deviations from the x and y direction simultaneously. This avoids the common and incorrect practice of first building a regression model which minimizes the y deviations for a given level of x and then using this model to predict x for a given level of y. The method of calculating m and c are from Cohen, 1980, and will be referred to as an invertible linear regression.

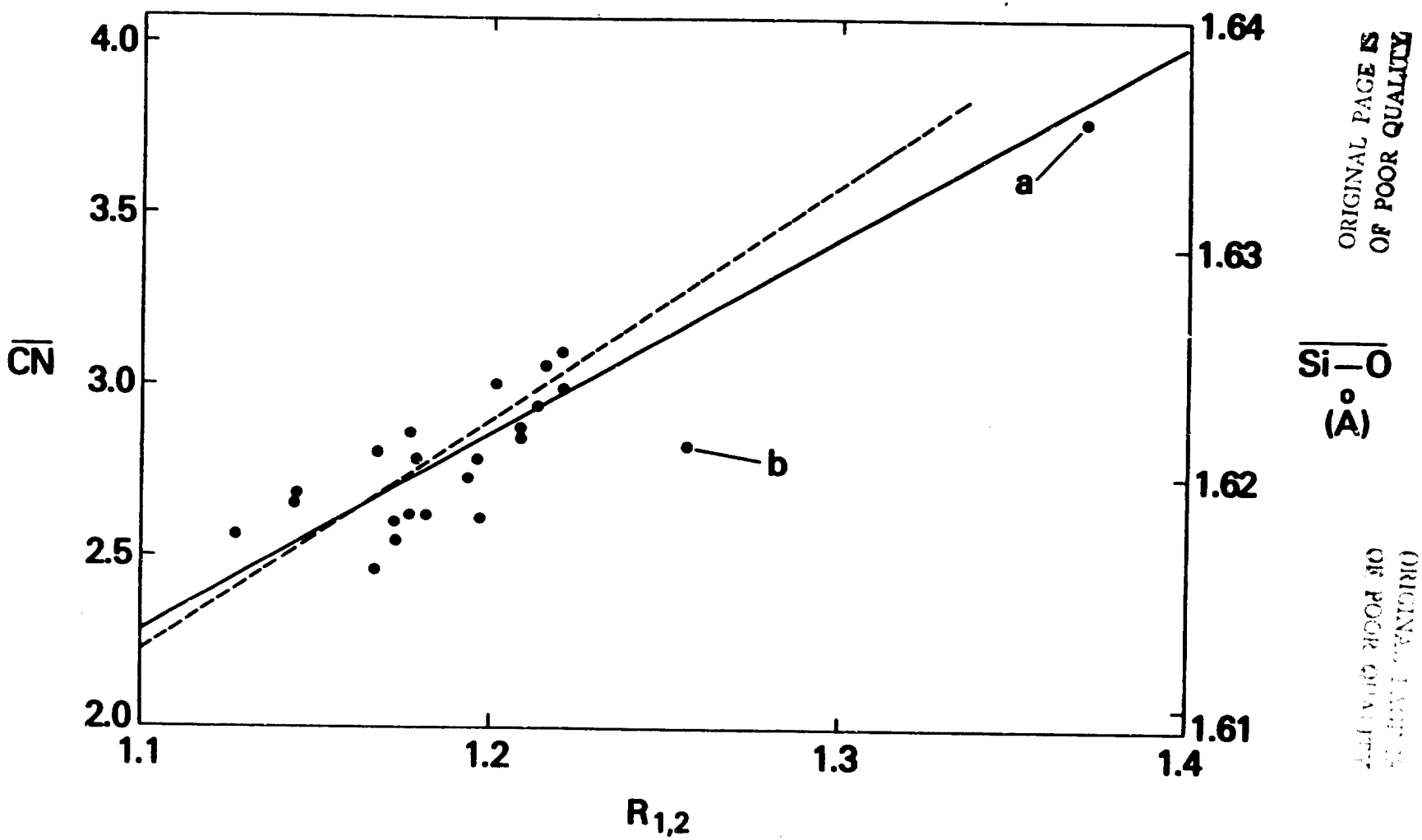

Figure 2. Average Oxygen Coordination Number ($\overline{CN}$) Plotted Against Ratio of Intensities in Two Thermal Infrared Bands ($R_{1,2}$). Solid line ——— all 25 samples; dashed line – – – – all samples except peridotite (a) and anorthosite (b). Si–O distance, $\overline{Si–O}$, calculated on the basis of $\overline{CN}$ is also given on the ordinate.

appear in Table 9.[3] The interpretation of these is that Si–O bond distance, which is related to Si–O bond strength and polymerization of Si, is probably the major cause of the shift in the position of the emittance depression.

Table 9
Invertible linear regression (using method of Cohen, 1980) between $R_{1,2}$ and average coordination number (CN): ($R_{1,2} = mCN + c$).

	m	c	r
All 25 Samples	0.177	0.692	0.86
Without Sample 26 (Peridotite)	0.127	0.832	0.68
Without Sample 24 (Anorthosite)	0.173	0.703	0.89
Without Samples 24 and 26	0.149	0.768	0.74

[3]The value of r in Tables 9 and 10 will vary depending on whether or not samples 24 (anorthosite) and 26 (peridotite) are included in the analysis. The impact of these samples upon r can be seen by examining the following equations: $r^2 = 1 - SSE/SSTO = SSR/SSTO$, where $r = \sqrt{r^2}$ and SSTO = SSR + SSE. The position of these points (samples 24 and 26) relative to the rest of the points will determine which of the terms SSE or SSR (along with SSTO) will be increased. In the case of sample 26, because there are no other points in its range of x and y values, it will have a large impact on the regression line, causing the line to pass close to the point. Thus, while we are increasing SSTO, most of the increase is explained by the regression (SSR). This will produce an increase in r^2 and hence in r. Alternatively, there are a number of x values in the same range as the x value of sample 24. Thus, the impact upon the regression of sample 24 is much diluted and so while there is an increase in SSTO, most of the increase is in the error term (SSE). This situation will produce a decrease in r^2 and r. From a statistical viewpoint, the anorthosite is an outlier. Further appropriateness of the regression should not depend upon inclusion of the peridotite. The reader, however, is presented with the results of four regressions to allow consideration of all combinations for including samples 24 and 26.

CONCLUSIONS

A theoretical basis for the empirical relationship between the position of the thermal infrared emittance depression exhibited by silicate igneous rocks has been established as being due to the change in the average Si–O bond strength and distance with increased average degree of polymerization of SiO_4 tetrahedra of the silicate mineral constituents.

Interestingly, the trend of increased polymerization toward tectosilicates (quartz and feldspar) is the same trend observed in the crystal fractionation of igneous rocks. The evolution of rocks in a magmatic series is generally marked by increased concentrations of normative quartz and alkali feldspars. On this basis, Thornton and Tuttle (1960) proposed the use of a quantitative measure of chemical differentiation which can be used for the classification of igneous rocks. The Differentiation Index (DI) is defined as the amount (in weight percent) of normative quartz + orthoclase + albite + nepheline + leucite + kalsilite. Thornton and Tuttle point out that, "no more than three of these normative minerals will appear in any given norm. Thus, the Differentiation Index is simply the sum of the percentages of the three normative minerals". In applying the DI to chemical analyses for representative major igneous rocks, the authors obtained the following values:

Intrusive Rock Type	DI	Extrusive Rock Type	DI
Alkali Granite	93	Alkali Rhyolite	91
Granite	80	Rhyolite	88
Granodiorite	67	Quartz Latite	68
Diorite	48	Andesite	66
Gabbro	30	Basalt	35
Olivine Gabbro	27	Olivine Diabase	30
Peridotite	6	Picrite	12

The Differentiation Indices for the rock suite used in this work are plotted against $R_{1,2}$ in Figure 3 and statistics are given in Table 10. The DI's for the major intrusive rock types are noted on the ordinate. (In view of the location of sample a, the peridotite, the use of a second-order equation would significantly improve the correlation. However, there is no theoretical basis to justify this step.)

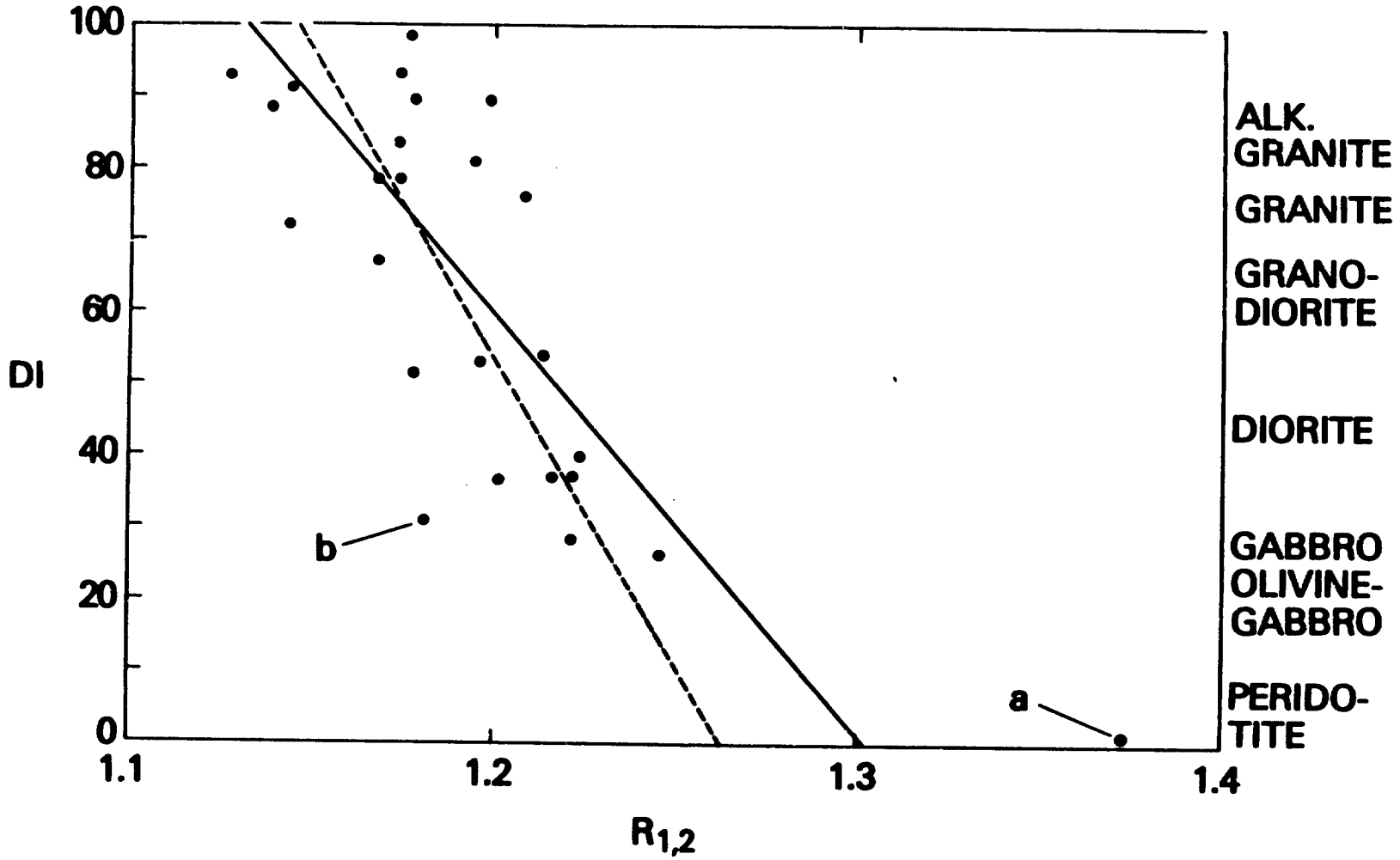

Figure 3. Differentiation Index (DI) plotted against ratio of intensities in two thermal infrared bands ($R_{1,2}$). Solid line ——— all 25 samples; dashed line — — — all samples except peridotite (a) and anorthosite (b). Intrusive rock types corresponding to DI values are indicated on the ordinate.

Table 10
Invertible linear regression (using method of Cohen, 1980) between differentiation index (DI) and $R_{1,2}$: ($R_{1,2} = mDI + c$).

	m	c	r
All 25 Samples	-0.00172	1.302	-0.74
Without Sample 26 (Peridotite)	-0.00120	1.270	-0.68
Without Sample 24 (Anorthosite)	-0.00174	1.309	-0.72
Without Samples 24 or 26	-0.00116	1.262	-0.63

The relationship on which Figure 3 is based appears to combine the fundamental causative principles behind the variation in the position of the emittance depression and those of igneous rock petrogenesis and classification. It may, therefore, be the most appropriate relationship for classification of rocks by remote sensing using this portion of the electromagnetic spectrum.

One of the problems, however, in interpreting Vincent's data lies in the selection of the spectral bands used to determine $R_{1,2}$; the overlap between the bands undoubtedly weakens the sensitivity of $R_{1,2}$ to the rock composition variable. Based on theoretical considerations and analyses of thermal infrared spectra of 134 rocks, Holmes and Nuesch (1978) proposed three improved spectral bands for rock discrimination in the thermal infrared region of the spectrum. These bands are: 8.1 – 9.1, 9.5 – 10.5 and 11.0 – 12.0 μm. The use of these bands would probably improve upon the correlations obtained in this paper.

It is interesting to note that the relationship between average Si-O bond distance and the position of the emittance depression is independent of the texture of the rock. This is probably because the degree of polymerization is a statistical relationship based on the abundance of silicon relative to other cations; this relationship may well hold whether the material is crystalline or glassy.

While the evidence for the relationship between the position of the emittance minimum and the average Si–O bond distance is rather compelling, the authors would feel more comfortable, especially concerning the quantitative aspects of the relationships, if additional laboratory observations were available. We suggest that a significantly larger set of samples be analyzed. Indeed a great deal of the correlation we see rests on one sample, the peridotite, and there is a considerable hiatus from the next most basic rock (the gabbro at $R_{1,2} = 1.24$) to the peridotite ($R_{1,2} = 1.372$). Although rocks which fall between gabbroic and peridotitic compositions are rare, some samples should be found and analyzed to fill this void.

ACKNOWLEDGMENTS

The authors wish to acknowledge the able and constructive critical review of the manuscript by several of their co-workers, Drs. Robert Belcher, Paul Lowman and Robert Price. We wish to thank Dr. Robert Vincent for kindly permitting us to use his data (Table 1). One of the authors (L. W.) especially appreciates the guidance of Prof. G. V. Gibbs in the crystal chemical interpretation. On the other hand, the authors accept full responsibility for any possible errors of deficiencies in this work.

REFERENCES

Brown, C. E. and Gibbs, G. V., 1969, Oxygen coordination and the Si–O bond, Amer. Min., v. 54, p. 1528–1539.

Chayes, F., 1971, Ratio Correlation, Univ. of Chicago Press, Chicago, 99 pp.

Cohen, S. C., 1980, Relationship Among the Slopes of Lines Derived from Various Data Analysis Techniques and the Associated Correlation Coefficient, TM 80722, National Aeronautics and Space Administration, Greenbelt, MD., 3 pp.

Daniel, C., and Wood, F. S., 1971, Fitting Equations to Data, Wiley-Interscience, John Wiley and Sons, Inc., New York, 342 pp.

Draper, N. R. and Smith, H., 1966, Applied Regression Analysis, Wiley-Interscience, John Wiley and Dons, Inc., New York, 407 pp.

Farmer, V. C., 1974, Orthosilicates, pyrosilicates and other finite chain silicates, *in:* The Infrared Spectra of Minerals, V. C. Farmer, ed., Min. Soc. Mono., v. 4, London, p. 285-304.

Fisher, R. A., 1970, Statistical Methods for Research Workers, 14th ed., Hafner Press, New York, 362 pp.

Frane, J., 1979, All possible subsets regression, *in:* BMDP Biomedical Computer Program, P-Series, W. J. Dixon and M. B. Brown, eds., Univ. of California Press, Berkeley, Calif., p. 418-436.

Furvival, G. M. and Wilson, Jr., R. W., 1974, Regression by leaps and bounds. Technometrics, v 16, no. 4, p. 499-511.

Gorsuch, R. L., 1974, Factor Analysis, W. B. Saunders Co., Phila., PA., 730 pp.

Holmes, Q. A. and Nuesch, D. R., 1979, Optimum thermal infrared bands for mapping general rock type and temperature from space: Environmental Institute of Michigan Fianl Report No. 130100-13-F on Contract No. NAS9-15362 (Johnson Space Center, Houston, TX).

Karr, Jr., C., ed., 1975, Infrared and Raman Spectroscopy of Lunar and Terrestrial Minerals, Academic Press, New York, 375 pp.

Kim, J., 1975, Factor analysis, *in:* Statistical Package for the Social Sciences, N. H. Nie, C. H. Hull, J. G. Jenkins, J. Stenbrenner, D. H. Bent, eds., McGraw-Hill Book Co., New York, p. 468-514.

Kovach, J. J., Hiser, A. L. and Karr, C., Jr., 1975, Far infrared spectroscopy of minerals, *in:* Infrared and Raman Spectroscopy of Lunar and Terrestrial Minerals, C. Karr, Jr., ed., Academic Press, New York, p. 231-254.

Logan, L. M., Hunt, G. R. and Salisbury, J. W., 1975, The use of mid-infrared spectroscopy in remote sensing of space targets, *in:* Infrared and Raman Spectroscopy of Lunar and Terrestrial Minerals, C. Karr, Jr., ed., Academic Press, New York, p. 117-142.

Lyon, R. J. P., 1964, Evaluation of Infrared Spectrophotometry for Compositional Analysis of Lunar and Planetary Soils: Rough and Powdered Surfaces, Final Report, Part 2, NASA Report CR-100, 115 pp.

Lyon, R. J. P., and Green, A. A., 1975, Reflectance and emittance of terrain in the mid-infrared (6-26 μm) region, *in:* Infrared and Raman Spectroscopy of Lunar and Terrestrial Minerals, C. Karr, Jr., ed., Academic Press, New York, p. 165-195.

Neter, J. and Wasserman, W., 1974, Applied Linear Statistical Models, Richard D. Irwin, Inc., Homewood, Ill., 842 pp.

Rogers, K. A., Cochrane, R. H. A. and LeConteur, P. C., 1970, Fortran II and Fortran IV programs for petrochemical calculations, Min. Mag., v. 37, p. 952-953.

Ryan, Jr., T. A., Joiner, B. L. and Ryan, B. F., 1976, Minitab II Reference Manual, Computation Center, Penn State Univ., University Park, PA., 100 pp.

Smith, J. V. and Bailey, S. W., 1963, A second review of Al-O and Si-O tetrahedral distances, Acta Crystall., v. 16, p. 801-811.

Smith, W. L., 1977, Remote Sensing Applications for Mineral Exploration, Dowdin, Hutchinson and Ross, Stroudsburg, PA, 391 pp.

Strens, R. G. J., 1974, The common chain, ribbon and ring silicates, *in:* The Infrared Spectra of Minerals, V. C. Farmer, ed., Min. Soc. Mono., v. 4, London, p. 305-330.

Thornton, C. P. and Tuttle, O. F., 1960, Chemistry of igneous rocks: I. Differentiation index, Am. J. Sci., v. 258, p. 664-684.

Vincent, R. K., 1973, A Thermal Infrared Ratio Imaging Method for Mapping Compositional Variations Among Silicate Rock Types, Ph. D. Thesis, U. Michigan, Ann Arbor, 102 pp.

Vincent, R. K. and Thompson, F., 1972, Spectral compositional imaging of silicate rocks, Jour. Geoph. Res., v. 77, p. 2465-2472.

Walter, L. W., Blodget, H. and Schutt, J., 1976, Satellite and laboratory spectral measurements of rock compositional variations, Am. Geophys. Union, Trans., *57*, p. 1014.

FIGURE CAPTIONS

Figure 1. Individual 95 Percent Confidence Interval for Group Means (Based on Pooled Standard Deviations).

Figure 2. Average Oxygen Coordination Number (CN) Plotted Against Ratio of Intensities in Two Thermal Infrared Bands ($R_{1,2}$). Solid line———all 25 samples; dashed line-------all samples except peridotite (a) and anorthosite (b). Si-O distance, Si-O, calculated on the basis of CN is also given on the ordinate.

Figure 3. Differentiation Index (DI) Plotted Against Ratio of Intensities in Two Thermal Infrared Bands ($R_{1,2}$). Solid——— all 25 samples; dashed line-------- all samples except peridotite (a) and anorthosite (b). Intrusive rock types corresponding to DI values are indicated in the ordinate.

BIBLIOGRAPHIC DATA SHEET

1. Report No. 82019	2. Government Accession No.	3. Recipient's Catalog No.
4. Title and Subtitle A Physical Basis for Remote Rock Mapping of Igneous Rocks Using Spectral Variations in Thermal Infrared Emittance		5. Report Date 6. Performing Organization Code 920
7. Author(s) Louis S. Walter and Mark L. Labovitz		8. Performing Organization Report No.
9. Performing Organization Name and Address Applications Directorate NASA/Goddard Space Flight Center Greenbelt, Maryland 20771		10. Work Unit No. 11. Contract or Grant No. 13. Type of Report and Period Covered TM
12. Sponsoring Agency Name and Address Same as Above		14. Sponsoring Agency Code
15. Supplementary Notes		

16. Abstract

The thermal infrared spectra of rocks are potentially of considerable importance for remote sensing. This paper presents results of a theoretical investigation of the relation between spectral features in the 8–12 micrometer region and rock type. Data on compositions of a suite of rocks and measurements of their spectral intensities in 8.2–10.9 and 9.4–12.1 micrometer bands published by Vincent (1973) were subjected to various quantitative procedures. It was found that there was no consistent direct relationship between rock group names and the relative spectral intensities. However, there is such a relationship between the Thornton–Tuttle (1960) Differentiation Index and the relative spectral intensities. This relationship is explicable on the basis of the change in average Si–O bond length which is a function of the degree of polymerization of the SiO_4 tetrahedra of the silicate minerals in the igneous rocks.

17. Key Words (Selected by Author(s))	18. Distribution Statement		
Remote Sensing Rock Mapping Thermal Infrared			
19. Security Classif. (of this report)	20. Security Classif. (of this page)	21. No. of Pages	22. Price*
Unclassified	Unclassified		

*For sale by the National Technical Information Service, Springfield, Virginia 22161.